

## Moving temporary wall in microfluidic devices

Vahid Bazargan<sup>1,\*</sup> and Boris Stoeber<sup>1,2</sup>

<sup>1</sup>*Department of Mechanical Engineering, University of British Columbia, Vancouver, British Columbia, Canada V6T 1Z4*

<sup>2</sup>*Department of Electrical and Computer Engineering, University of British Columbia, Vancouver, British Columbia, Canada V6T 1Z4*

(Received 6 June 2008; published 4 December 2008)

This paper describes the formation of a temporary wall between two fluid streams in a microfluidic channel. Diffusion of ions from one fluid stream into a costreaming thermally responsive polymer solution is used to lower the local gelation temperature of the polymer, leading to formation of a gel wall in the center of the flow channel. The mechanisms driving either the generation or removal of the wall on its both sides are described and discussed. This wall allows well-controlled transport of particles from one stream into the other.

DOI: [10.1103/PhysRevE.78.066303](https://doi.org/10.1103/PhysRevE.78.066303)

PACS number(s): 47.61.Fg, 47.55.pd, 47.61.Jd

Microfluidics studies and uses fluid mechanics in small-scale environments [1]. Typical applications are in the biomedical field where, for instance, small amounts of biologically relevant sample are transported and manipulated on-chip. A simple and very effective microfluidic device is the so-called T sensor; here, diffusion of compounds from co-streaming fluids occurs across the flow channel, which results in fluorescence signals that allow measurement of the concentrations of compounds of interest [2]. This device takes advantage of the fluid behavior in microfluidic environments that is dominated by viscosity  $\mu$  at this small length scale  $L$  compared to inertia effects, and which is therefore characterized by a small Reynolds number  $Re=UL\rho/\mu\ll 1$ , with a characteristic flow velocity  $U$  and mass density  $\rho$  of the fluid.

The typical low-Reynolds-number flow regime in microfluidic systems offers the opportunity for fundamentally different flow control strategies compared to macroscopic flow systems. For instance, several flow control strategies based on hydrogels have been demonstrated in the past. Beebe and co-workers demonstrated hydrogel valves that were anchored inside a flow channel; upon change of the pH value of the surrounding fluid, the hydrogel would swell or collapse and thus block or open a flow passage [3]. Baldi and co-workers demonstrated a similar concept for a valve response to a change in glucose concentration [4]. These valve concepts rely on mass diffusion of compounds (with the mass diffusion constant  $D$ ) into the hydrogel matrix, which at the typically small length scales in microfluidic devices occurs at a small time scale  $t\sim L^2/2D$ .

In a different approach, Stoeber and co-workers developed a valve concept where a heat-sensitive polymer is transported with the fluid stream that can reversibly turn into a gel upon heating [5]. Targeted heating of the channel with small integrated heaters led to localized gel formation in the channel and subsequent channel blockage. Shirasaki and co-workers employed a similar valve concept while using infrared lasers for heating and subsequent formation of a hydrogel inside a microfluidic channel [6].

Here we present a simple concept for formation of a temporary separating wall between two co-streaming fluids in a

microfluidic device based on the thermally responsive hydrogel used in [5]. This wall results from the diffusion of compounds from one stream into the other, which can lead to gel formation at the interface between the two fluids. The gel wall can be removed at any time by lowering the device temperature by a few degrees.

One of the fluids is an aqueous solution of the biocompatible polymer Pluronic. These solutions undergo reversible gel formation at elevated temperature [5]. The gel formation temperature depends on the type of Pluronic and its concentration [7]. In many cases, a gel melting temperature exists above which the gel reversibly liquefies again. It is believed that this phase transition is due to an increasing dehydration of the poly-(ethylene oxide) block of the Pluronic molecules at elevated temperature, which eventually leads to a breakdown of the gel structure [9]. The addition of certain inorganic salts can also change the gel formation temperature, where for example the presence of sodium thiocyanate (NaSCN) leads to an increase of the gel formation temperature [8] and the addition of sodium chloride (NaCl) or sodium phosphate ( $\text{Na}_3\text{PO}_4$ ) decreases the temperature necessary for gelation [9]; at high concentrations of the gel-temperature-lowering salts, the gel formation capability of this fluid can be entirely lost [9]. In particular, it has been found that salts with di- and trivalent anions such as  $\text{Na}_3\text{PO}_4$  lower the gel melting temperature more dramatically than the gel formation temperature. In our system, the gel formation temperature and the gel melting temperature become effectively the same at a certain critical concentration of  $\text{Na}_3\text{PO}_4$ , which results in a loss of the gel formation ability of Pluronic 15 wt % at  $\text{Na}_3\text{PO}_4$  concentrations above this critical concentration [9]. The influence of sodium phosphate ( $\text{Na}_3\text{PO}_4$ ) on the gel formation behavior of an aqueous solution of 15 wt % Pluronic F127 (from BASF) as shown in Fig. 1(a) has been determined with cone and plate viscometry. The temperature at which the viscosity of a particular solution increases significantly was identified as the respective gelation temperature  $T_G$ . Figure 1(b) shows  $T_G$  as a function of sodium phosphate concentration  $C_S$ ; the gelation temperature decreases from  $T_G=26.3^\circ\text{C}$  at  $C_S=0$  mol/l to  $T_G=19.9^\circ\text{C}$  at  $C_S=0.253$  mol/l. Above  $C_S=C_{S,\text{crit}}=0.253$  mol/l no gel formation was observed.

A Y-shaped microfluidic channel system (depth  $10\ \mu\text{m}$ , width  $500\ \mu\text{m}$ ) was fabricated using standard soft lithography [10]; after molding, the surface of structured poly-

\*vbazarg@interchange.ubc.ca

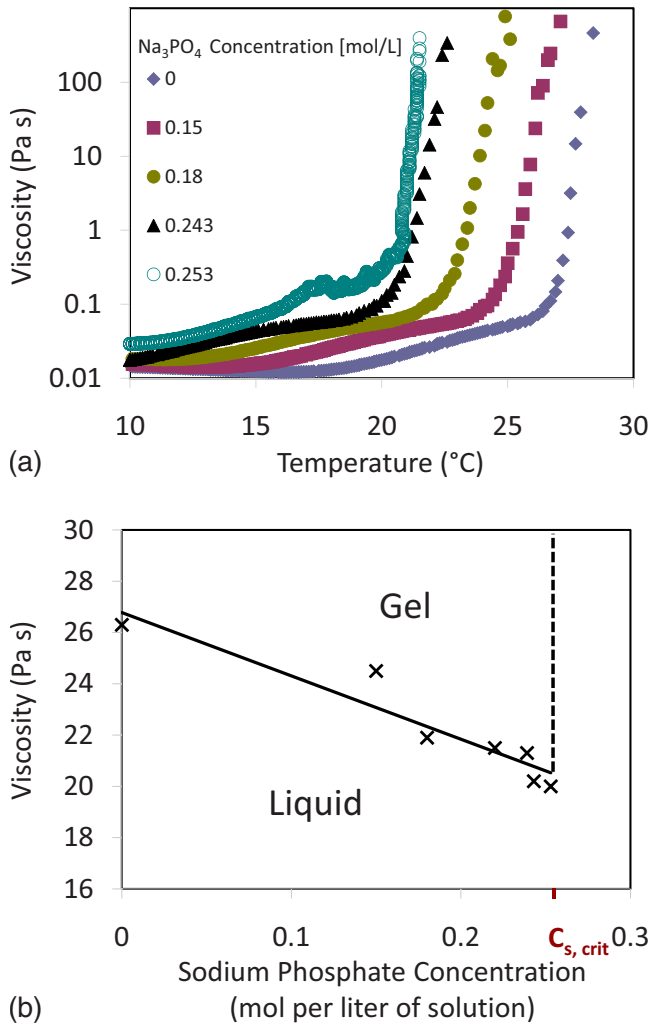


FIG. 1. (Color online) Influence of sodium phosphate on the gel formation behavior of a 15 wt % Pluronic F127 solution. (a) Viscosity of the Pluronic solution as a function of temperature for different concentrations  $C_S$  of sodium phosphate in the Pluronic solution from cone and plate viscometry at controlled shear stress (0.6 Pa). The temperature at which the measured viscosity increases significantly can be identified as the gel formation temperature  $T_G$ . (b) Gel formation temperature  $T_G$  of the Pluronic solution from (a) as a function of sodium phosphate concentration  $C_S$ .

(dimethylsiloxane) was bonded to a glass slide. Solutions of both Pluronic (15 wt %) and sodium phosphate (0.5–1.0 mol/l) were prepared using distilled water. Carboxylated 0.51- $\mu\text{m}$ -diameter fluorescent polystyrene microspheres (fluoresbrite by Polysciences, Inc.) at a concentration of 0.02 wt % were used in these solutions for flow visualization. The fluorescent dye rhodamine B from (Sigma-Aldrich Co.) was mixed into one of the streams and used to evaluate diffusion. The fluids were driven at controlled pressure using an eight-channel pressure source MFCS-8C 1000 by Fluigent. The flow was observed with the inverted stage epifluorescence microscope TE2000U by Nikon and an Imager Pro X 2M particle image velocimetry (PIV) camera. PIV was performed using the DAVIS software package version 7.2.1.27 by LaVision.

The two fluids were introduced into the microfluidic de-

vice as shown in Fig. 2(a) and were driven at a constant pressure. The entire device was at ambient temperature (24 °C) without heating or cooling any particular part of the device. As sodium phosphate diffuses into the Pluronic stream, it lowers the gel formation temperature below the ambient temperature and leads to gel formation along the center of the main flow channel. Seed particles trapped in this wall appear sharp, whereas the streak images of the seed particles in the Pluronic solution indicate fast flow. The velocity profiles of both Pluronic solution and sodium phosphate solution were measured using particle image velocimetry [Fig. 2(b)]. Since the Pluronic solution has a much higher viscosity than the saline solution, the velocity of the Pluronic solution is much lower. Therefore, both PIV measurements were performed separately to achieve a higher accuracy.

The velocity profile of the Pluronic solution is asymmetric with a lower velocity near the gel wall. This lower velocity indicates a higher viscosity of the Pluronic solution near the gel wall and according to Fig. 1(a) this higher viscosity is caused by sodium phosphate diffusing into the Pluronic solution. Lacking any means to measure the concentration of sodium phosphate at a high spatial resolution in all locations of the microfluidic systems in a noninvasive way, a low concentration of the fluorescent dye rhodamine B was used as a sample compound to evaluate cross-channel diffusion. The dye was introduced into the saline stream. The fluorescence intensity in the channel is observed, which correlates with the dye concentration. The size of a rhodamine molecule is comparable to that of sodium phosphate with molecular weights of 479 and 164 Da, respectively, and their diffusion constants in aqueous solution at 24 °C are comparable with  $5 \times 10^{-6}$  [11] and  $6 \times 10^{-6}$  cm<sup>2</sup>/s [12], respectively. Figure 2(c) shows the fluorescence brightness of rhodamine B across the flow channel; the dye is about 3.2 times brighter in Pluronic solution than in saline solution, and it is two times brighter in the Pluronic solution compared to the gel, as verified through experiments. Correlating the fluorescence brightness with the concentration of rhodamine B and with the concentration of sodium phosphate in the system yields a sodium phosphate concentration of around 0.1 mol/l at the edge of the gel wall and the Pluronic stream. This value corresponds to the sodium phosphate concentration necessary for gel formation at  $T=24$  °C in the phase diagram in Fig. 1(b). The decreasing amount of fluorescence in the Pluronic solution further away from the wall correlates well with the velocity profile in Fig. 2(b) as discussed above. Because of the much higher molecular weight of the Pluronic molecules (above 12 kDa) diffusion of Pluronic into the saline stream will be neglected in the following discussion.

Steady diffusion of sodium phosphate toward the Pluronic stream will increase the sodium phosphate concentration of the gel wall near the saline stream above the critical concentration  $C_{S, \text{crit}}$  so that the gel has to turn liquid at this location. Simultaneously, continuous diffusion of sodium phosphate across the wall and into the Pluronic solution will increase the concentration of sodium phosphate in the Pluronic stream near the wall to above the concentration threshold for gel formation according to Fig. 1(b). This means that the gel wall is constantly being dissolved on the side that is in con-

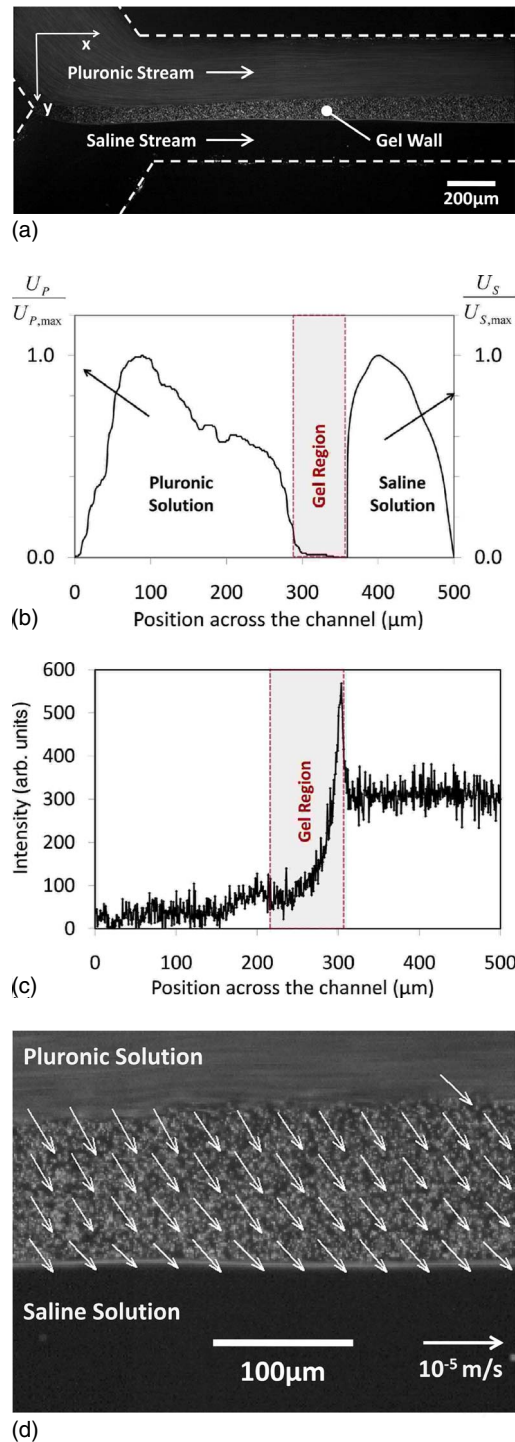


FIG. 2. (Color online) Formation of a gel wall along the center of a microfluidic channel. (a) The gel wall is formed between a Pluronic solution (top) with fluorescent seed particles and a sodium phosphate solution (bottom) without seed particles. (b) Flow velocity profiles from PIV at  $x=1.5$  mm, normalized separately for the Pluronic solution and the sodium phosphate solution with the flow rates of 3 and 30  $\mu\text{l/h}$ , respectively. (c) Fluorescence intensity of rhodamine B diffusing from the saline solution across the gel wall into the 15 wt % Pluronic F127 solution,  $C_S=1$  mol/l, at  $x=3$  mm from the entrance; rhodamine concentration in the saline solution, 0.3 g/l. (d) Velocity field showing the motion of the gel wall; a larger image with more detail can be found in [13].

tact with the saline stream, and gel is constantly generated on the side of the wall that is in contact with the Pluronic stream. As a consequence, the wall can only have a fixed position in the channel if the gel that constitutes the wall moves across the channel. This slow motion of the wall is shown by the vector field from PIV in Fig. 2(d), and the motion of the system is well illustrated by the movie and PIV measurements in [13]. The PIV measurement of the velocity of the wall reveals steady motion at nearly constant velocity  $v_y=5$   $\mu\text{m/s}$  along the channel from the Pluronic stream toward the saline stream. It also shows increasing velocity in the direction of the fluid streams along the channel; this is most likely induced by the viscous forces of the fluid streams acting on the wall, which increases slightly in width along the channel. The cross channel velocity  $v_y$  is insensitive to the velocity of the fluids. This indicates a constant gel removal rate by the saturated saline solution near the gel wall along the entire channel, which is maintained by the sufficiently high flow velocity of the saline solution. The position of the wall is constant for steady-state flow conditions, which indicates that the motion of the gel across the channel is not caused by a pressure difference between the two fluid streams. The cross-channel motion toward the saline stream has been observed for different pressures driving the two streams where either the pressure driving the Pluronic stream or the pressure driving the saline solution was higher.

Experiments show that at steady state the wall thickness increases by only a small amount along the investigated channel length of 1.5 mm, while the wall thickness  $W$  was in the range 50–200  $\mu\text{m}$  depending on the experimental conditions. With a fixed sodium phosphate concentration on either side of the wall and a relatively constant wall thickness, the flux of sodium phosphate across the wall is constant along the channel, and the edge of the wall in contact with the Pluronic solution can be considered a constant source of sodium phosphate. Diffusion of ions into a Pluronic solution with an ion concentration just below the gel formation concentration will lead to gel formation and advancement of the gel in direction of the Pluronic stream. This propagation of the gel wall through mass diffusion can be investigated through the equivalent heat diffusion problem, where temperature  $T$  is equivalent to concentration  $C_S$  and heat flux  $q$  corresponds to molecular flux  $\Phi$ . The temperature distribution  $T(x)-T_0 \sim q\sqrt{x}/U_0$  along a plate  $T(x) \sim q$  that provides a constant heat flux  $q$  into the fluid depends on the location  $x$ , the free stream velocity  $U$  and a reference temperature  $T_0$  [14]. This corresponds to an increasing sodium phosphate concentration at the wall surface along the channel. However, if this concentration becomes higher than  $C_{S,crit}$ , there will be a location in the channel close to the wall with  $C=C_{S,crit}$ , and the region between the original wall surface and this location should have solidified to gel.

In the equivalent thermal problem, this location scales as the thermal boundary layer for the case of forced convection in laminar flow over a flat plate with a known wall temperature. The assumption of a thermal (or concentration) boundary layer much smaller than the velocity boundary layer (which here spans the entire channel) is justified by the concentration profile in the Pluronic stream from Fig. 2(c). The thermal boundary layer  $\delta_T \sim \sqrt{x/U}$  of a wall with constant



temperature depends through the local Reynolds number  $Re_x$  on location  $x$  and the free-stream (or average) velocity  $U$  of the Pluronic solution [15]. This thermal boundary layer thickness relates to the mass diffusion problem considered in the form of a mass diffusion length. For the expected small changes of the concentration at the location of the original wall surface along the channel, we assume it is justified to superimpose the results for concentration increase and the diffusion length for constant concentration at the boundary. This is also justified by the relatively large wall thickness compared to the thickness changes along the channel. For the equivalent thermal problem we therefore find a thermal boundary layer thickness  $\delta_T' \sim q\sqrt{x}/U\sqrt{x}/U = qx/U$  that is proportional to the heat flux at the wall,  $q$ , and to the location along the channel,  $x$ , while it is inversely proportional to the free-stream velocity  $U$ .

If we interpret the increase of this thermal boundary layer along the channel as an increase in the wall thickness  $\delta_C \sim \Phi x/U$  for the mass diffusion problem, then this result correlates very well with our experimental observations. The wall thickness increases linearly along the channel as shown in Fig. 2(a), and the increase in thickness  $\alpha_w \sim d\delta_C/dx \sim \Phi/U$  is proportional to  $1/U$  as confirmed by the data in Fig. 3(a), assuming that in the viscous limit of our experiments the pressure driving the fluid  $p$  is proportional to the corresponding flow rate  $Q$  or the flow velocity  $U$ . In addition, if we assume that the molecular flux  $\Phi$  is proportional to the sodium phosphate concentration in the saline stream  $C_{S0}$ , then the change in wall thickness  $\alpha_w$  has to be proportional to  $C_{S0}$ , as shown in Fig. 3(b).

Knowledge of the effect of sodium phosphate on the gel formation of Pluronic solutions and an understanding of mass diffusion in microfluidic environments are sufficient for a physical understanding of the dynamics of the observed wall formation in microfluidic channels. While this mechanism allows the formation of a temporary wall separating two fluid streams, this wall also serves as a vehicle to slowly transport entities from one stream into the other stream. This transport principle could be applied to cells that slowly move from one stream through the wall along a concentration gradient into a medium of elevated concentration of certain ions, so that the cells would have sufficient time to adapt.

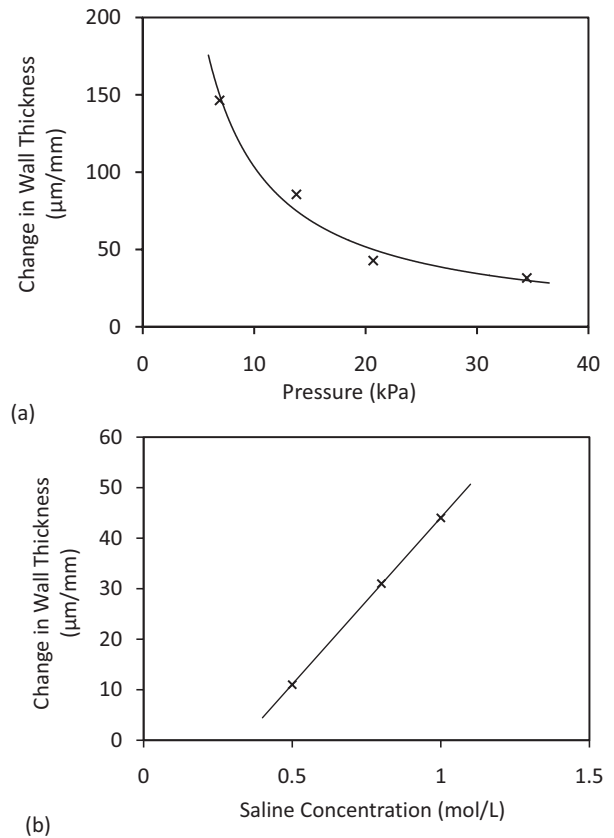


FIG. 3. Change of the gel wall thickness per length along the channel  $\alpha_w$  as a function of (a) the pressure  $p$  driving the fluids and (b) the sodium phosphate concentration  $C_{S0}$ . The solid lines show curve fits to (a)  $\alpha_w = a_1 p^{-1}$  and (b)  $\alpha_w = a_2 C_{S0} + a_3$ .

Since the cross-channel transport velocity of the wall,  $v_y$ , is constant, and the wall thickness can be varied through the flow velocity of the fluid streams, the temporal concentration gradient  $dC_S/dt$  that objects experience as they move across the wall can be selected through the flow velocity of the two streams.

This research was supported by funding from the Natural Sciences and Engineering Research Council of Canada.

- [1] T. M. Squires and S. R. Quake, *Rev. Mod. Phys.* **77**, 977 (2005).  
 [2] B. H. Weigl and P. Yager, *Science* **283**, 346 (1999).  
 [3] D. J. Beebe, J. S. Moore, J. M. Bauer, Q. Yu, R. H. Liu, C. Devadoss, and B. H. Jo, *Nature (London)* **404**, 588 (2000).  
 [4] A. Baldi, Y. D. Gu, P. E. Loftness, R. A. Siegel, and B. Ziaie, *J. Microelectromech. Syst.* **12**, 613 (2003).  
 [5] B. Stoeber, Z. Yang, D. Liepmann, and S. J. Muller, *J. Microelectromech. Syst.* **14**, 207 (2005).  
 [6] Y. Shirasaki, J. Tanaka, H. Makazu, K. Tashiro, S. Shoji, S. Tsukita, and T. Funatsu, *Anal. Chem.* **78**, 695 (2006).  
 [7] B. Stoeber, C.-M. J. Hu, D. Liepmann, and S. J. Muller, *Phys. Fluids* **18**, 053103 (2006).  
 [8] M. Malmsten and B. Lindman, *Macromolecules* **25**, 5440 (1992).  
 [9] N. K. Pandit and J. Kisaka, *Int. J. Pharm.* **145**, 129 (1996).  
 [10] D. C. Duffy *et al.*, *Anal. Chem.* **70**, 4974 (1998).  
 [11] S. A. Rani, B. Pitts, and P. S. Stewart, *Antimicrob. Agents Chemother.* **49**, 728 (2005).  
 [12] T. S. Wiedemann, H. Herrington, C. Deye, and D. Kallick, *Pharm. Res.* **18**, 1489 (2001).  
 [13] See EPAPS Document No. E-PLLEE8-78-153811 for a movie showing the fluid dynamics of a gel wall in a microfluidic channel and PIV measurements showing the motion of the wall. For more information on EPAPS, see <http://www.aip.org/pubservs/epaps.html>.  
 [14] W. M. Rohsenow and H. Choi, *Heat, Mass, and Momentum Transfer* (Prentice-Hall, Englewood Cliffs, NJ, 1961).  
 [15] A. Bejan, *Heat Transfer* (Wiley, New York, 1993).